JACS
JOURNAL OF THE AMERICAN CHEMICAL SOCIETY

Article

pubs.acs.org/JACS

Relative Stability of Empty Exohedral Fullerenes: π Delocalization versus Strain and Steric Hindrance

Yang Wang,*[†,‡] Sergio Díaz-Tendero,[†,‡,¶] Manuel Alcamí,[†,‡,§] and Fernando Martín*[†,§,¶]

[†]Departamento de Química, Módulo 13, Universidad Autónoma de Madrid, 28049 Madrid, Spain
[‡]Institute for Advanced Research in Chemical Sciences (IAdChem), Universidad Autónoma de Madrid, 28049 Madrid, Spain
[¶]Condensed Matter Physics Center (IFIMAC), Universidad Autónoma de Madrid, 28049 Madrid, Spain
[§]Instituto Madrileño de Estudios Avanzados en Nanociencia (IMDEA-Nanociencia), 28049 Madrid, Spain

Supporting Information

ABSTRACT: Predicting and understanding the relative stability of exohedral fullerenes is an important aspect of fullerene chemistry, since the experimentally formed structures do not generally follow the rules that govern addition reactions or the making of pristine fullerenes. First-principles theoretical calculations are of limited applicability due to the large number of possible isomeric forms, for example, more than 50 billion for $C_{60}X_8$. Here we propose a simple model, exclusively based on topological arguments, that allows one to predict the relative stability of exohedral fullerenes without the need for electronic structure calculations or geometry optimizations. The model incorporates the effects of π delocalization, cage strain, and steric hindrance. We show that the subtle interplay between these three factors is responsible for (i) the formation of non-IPR (isolated pentagon rule) exohedral fullerenes in contrast with their pristine fullerene counterparts, (ii) the appearance of more pentagon−pentagon adjacencies than predicted by the PAPR (pentagon-adjacency penalty rule), (iii) the changes in regioisomer stability due to the chemical nature of the addends, and (iv) the variations in fullerene cage stability with the progressive addition of chemical species.

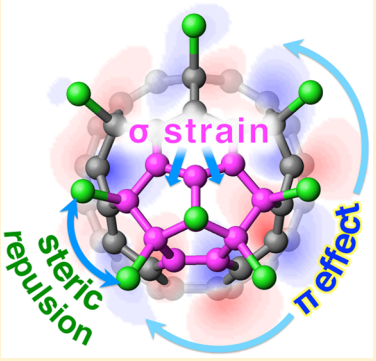

INTRODUCTION

Exohedral functionalization of fullerenes is the starting point for the synthesis of complex fullerene derivatives and nanodevices[1,2] with important implications in medicine[3−5] and materials science.[6−9] In medicine, exohedral fullerene derivatives are currently being tested as possible agents against HIV,[10−12] neurodegeneration,[13] ischemia,[14] osteoporosis,[15] general inflammation,[16] and the Ebola virus.[17] In materials science, they are used, for example, to manufacture donor−acceptor dyads[18−20] and efficient light-harvesting materials.[19,21] They have also shown a great potential for improving the performance of photovoltaic devices.[22,23]

Exohedral functionalization is usually accomplished by the binding of atomic or simple molecular species to the fullerene cage. The exohedral fullerenes thus produced, hereafter called *prototype* exohedral fullerenes, are found in many areas of science and have themselves interesting properties that are relevant to many applications.[24] Halogenated exohedral fullerenes, for instance, allow for nucleophilic substitution or addition of chemical species at specific fullerene sites[25−31] with a selectivity that is difficult to achieve in pristine fullerenes. Fluorofullerenes are known to have variable optical gaps[32] and, therefore, are ideal to produce selective light absorbers.[19,25,33,34] They have also been used as dopants to improve the surface conductivity of diamond[35] and as components of cathode materials for lithium batteries.[36,37] The simplest of all prototype exohedral fullerenes, hydrogenated fullerenes or fulleranes, are considered as potential carriers of diffuse interstellar bands and other interstellar and circumstellar features[38,39] and have been detected in meteorites.[40]

In the lab, prototype exohedral fullerenes are produced by arc-discharges,[41] combustion,[42,43] or radio frequencies.[44,45] These are high-temperature methods in which fullerene cages are formed through carbon-clustering processes (bottom-up growth), so that the resulting products usually correspond to the global energy minimum of the potential energy surface. Alternatively, they can also be synthesized in solution from existing pristine fullerene cages, as in hydrogenation,[46,47] halogenation,[48,49] and cycloaddition reactions.[50−55] These are low-temperature methods that usually preserve the original structure of the fullerene cage, so that the resulting products correspond to local minima of the potential energy surface.

A detailed description of the properties of prototype exohedral fullerenes can be found in several review articles.[56−62] Here we will focus on their relative stability and topology. It is well-known that exohedral fullerenes synthesized in a high-energy environment do not generally follow the rules that govern the relative stability of pristine fullerenes, such as the isolated pentagon rule (IPR)[63] and the pentagon adjacency

Received: November 10, 2016
Published: January 12, 2017

DOI: 10.1021/jacs.6b11669
J. Am. Chem. Soc. 2017, 139, 1609−1617

penalty rule (PAPR),[64,65] which favor the formation of fullerene cages in which pentagonal rings are separated from each other as much as possible. In fact, exohedral fullerenes containing non-IPR structures are more the rule than the exception.[66,67] Similarly, the addition patterns leading to the formation of the exohedral species do not generally follow the common principles of organic or inorganic synthesis.[68−70] Therefore, one of the main challenges in exohedral fullerene chemistry is to find reliable rules able to predict the structures found in experiments. This is the more so as the number of energetically accessible isomers is huge. For example, for a pristine fullerene such as C_{60}, the number of possible cage arrangements is as large as 1812, but the number of different ways a single cage can bind a given number of addends, say eight, is orders of magnitude larger: more than 20 million for the buckminsterfullerene cage. The combination of these two factors, number of cage isomers and addend distributions, makes the situation unmanageable. And it becomes even worse if one considers larger fullerene cages and more addends, since the number of cage isomers increases exponentially with the cage size and the number of possible addend distributions increases with the factorial of the number of addends. When the fullerene cage is initially predetermined, as in low-temperature experiments, the first of these numbers does not matter, but the second is still huge. In this scenario, ab initio quantum chemistry, density functional theory, and even semiempirical methods are obviously unpractical as prescreening tools to find the most stable structures.

Since the early days of fullerene research, some approximate rules have been proposed, but with limited applicability. Kroto and Walton[71] have shown that the stability of small C_nH_m ($n \leqslant 50$, $m \leqslant 10$) exohedral fullerenes increases with the number of conventional aromatic domains concomitant with alleviating cage strain. As a result of this, in some exohedral non-IPR fullerenes, only adjacent-pentagon sites are occupied in order to release the strain, for example, $C_{50}Cl_{10}$ and $C_{64}Cl_4$. However, this is not always the case, as for $C_{54}Cl_8$,[68] $C_{64}Cl_8$,[69] and $C_{50}X_{12}$ (X = H, F, Cl).[70] Fowler et al.[72,73] have pointed out that those addition patterns in which there is an odd number of bare carbon atoms isolated by addends have open-shell configurations and should be ruled out. Although this condition reduces the number of possible regioisomers, the reduction is not very important. Also, it has been proposed[73] that bulky addends, such as bromine, should never attach to adjacent carbon atoms on the fullerene cage. Using this assumption in combination with the above-mentioned closed-shell condition, Fowler et al. have been able to prescreen the relative stability of many regioisomers solely based on topological information.[73] However, the nonadjacent addition assumption is often violated, as for $C_{60}Br_6$,[74−76] $C_{60}(CF_3)_{14}$,[77] $C_{60}(CF_3)_{16}$,[78] $C_{70}(CF_3)_{18}$,[79] $C_{70}(CF_3)_{20}$,[80] etc. In contrast with the above, stepwise addition models appear as a promising alternative[70,81−88] supported by recent experiments on the chlorination of C_{74}.[89] In these models, one starts from a small set of known stable structures containing only a few addends and then more and more are incorporated in subsequent steps. Although this procedure substantially reduces the number of possible regioisomers and cage structures, it usually requires iterative electronic calculations and geometry optimizations at each addition step, which limits its applicability. Finally, genetic algorithms have also been applied in the search for minimum-energy exohedral fullerene isomers,[90] but they are computationally expensive and, therefore, are limited to small fullerene cages and a small number of addends.

In a recent work,[91] we have demonstrated that the relative isomer stability of endohedral metallofullerenes and charged fullerenes can be very easily predicted by using a pure topological model that is based on the concepts of cage connectivity and frontier π orbitals. The model thus avoids performing geometry optimizations or iterative electronic structure calculations. It has been successfully used to predict the experimentally observed structures of endohedral metallofullerenes, either IPR or non-IPR ones, among all possible isomers for a given fullerene size. In this paper, we present a generalization of this model to account for the change in π stability and steric effects that result from the binding of atomic or molecular species to the fullerene cage. We show that, in spite of the fact that the number of possible isomers is much larger than for pristine or endohedral fullerenes, the model works pretty well in predicting the cage topology and addends' distribution of the experimentally observed exohedral fullerenes. This is particularly useful when the synthesis is carried out in very hot environments, where chemical intuition is of little help and the number of energetically accessible isomers is orders of magnitude larger than for pristine fullerenes. The model also allows us to understand changes in the relative stability of the system due to changes in the number and nature of the addends. We thus conclude that the relative stability of exohedral fullerenes essentially results from the interplay between the stabilizing effect of π-electron delocalization and the destabilizing effects of strain and steric repulsion between addends.

THE EXOHEDRAL FULLERENE STABILIZATION INDEX (XSI) MODEL

As shown in ref 91, for pristine fullerenes of a given size $2n$, there is a linear correlation between the relative energy of the different isomers and the π stabilization energy, as given by the simple Hückel molecular orbital (HMO) theory. Here we extend this concept and assume that a similar linear correlation exists between the energy of the $[i, j]$ isomer of $C_{2n}X_{2m}$, where i denotes a particular cage isomer and j a particular regioisomer (i.e., a particular way of distributing the $2m$ addends on that cage), and its π energy referred to that of the ith isomer of pristine C_{2n}. According to HMO theory, the latter can simply be written as

$$\Delta E^{\pi}_{i,j} = 2\sum_{k=1}^{n-m}(\alpha + \beta\chi^{j}_{k,i}) - 2\sum_{k=1}^{n}(\alpha + \beta\chi_{k,i}) \quad (1)$$

where α is the Coulomb integral, β is the resonance integral responsible for the π bonding between adjacent carbon atoms, and $\{\chi^{j}_{k,i}\}$ and $\{\chi_{k,i}\}$ are, respectively, the highest $(n-m)$ and n eigenvalues of the connectivity matrices $\{a\}^{(ij)}_{\mu\nu}$ and $\{a\}_{\mu\nu}$ associated with the $[i, j]$ isomer of $C_{2n}X_{2m}$ and the ith isomer of C_{2n}. The connectivity matrix elements are equal to 1 if carbon atoms μ and ν are bonded, and 0 otherwise. We note that, for $C_{2n}X_{2m}$, the $2m$ carbon atoms bonded to the X addends are excluded from the definition of the connectivity matrix, because they do not participate in the π bonding. Consequently, the corresponding sum in eq 1 contains $(n-m)$ terms instead of n. We also note that the resonance integral β is always negative and the contribution of the Coulomb term α to the energy is assumed to be the same for all $[i, j]$ isomers.

DOI: 10.1021/jacs.6b11669
J. Am. Chem. Soc. 2017, 139, 1609−1617

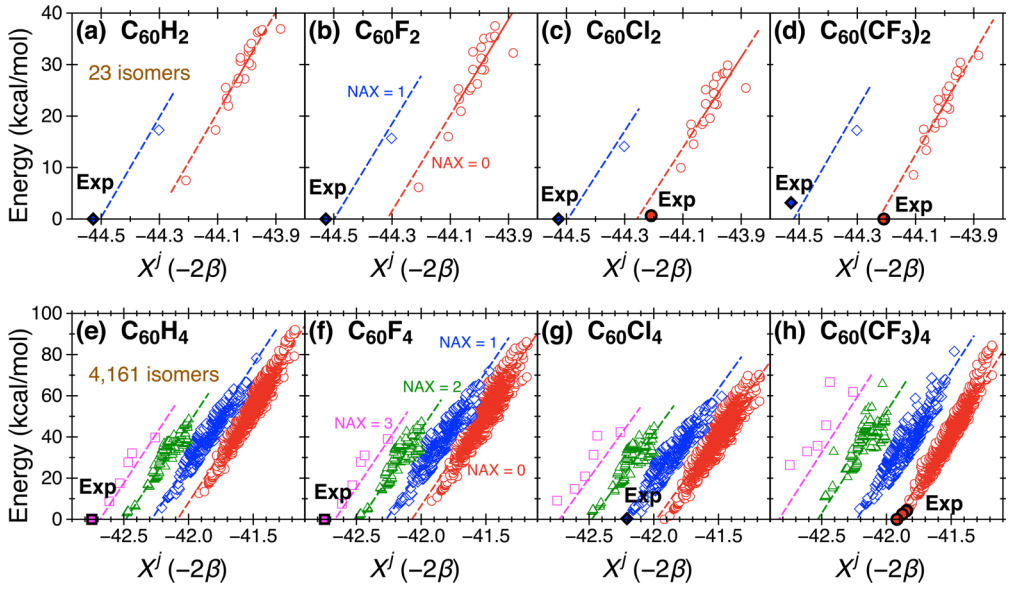

Figure 1. Correlation between relative DFTB energies and Hückel π stabilization energies, X_i^j, for all regioisomers j of exohedral fullerenes $C_{60}X_2$ (X = H, F, Cl, CF_3) (a–d) and $C_{60}X_4$ (e–h). All results are for isomers derived from the $I_h(1)$-C_{60} cage. Regioisomers are grouped according to the number of adjacent X groups (NAX) and indicated by different colors and symbols. Experimentally synthesized regioisomers[48,57,62,92] are highlighted by filled symbols. The total number of regioisomers is indicated in panels a and e.

Using $-2m\alpha$ as a reference energy value for all $[i, j]$ isomers of $C_{2n}X_{2m}$, one can simply write (in units of -2β)

$$X_i^j \equiv (\Delta E_{i,j}^{\pi} + 2m\alpha)/(-2\beta) = \sum_{k=1}^{n} \chi_{k,i} - \sum_{k=1}^{n-m} \chi_{k,i}^j \quad (2)$$

An illustration of the correlation between the X_i^j index and the relative DFTB (see Methods section) energies of the $C_{60}X_2$ and $C_{60}X_4$ isomers, for X = H, F, Cl, and CF_3, is shown in Figure 1. As can be seen, the correlation is very good in all cases. Interestingly, one can distinguish different correlation subgroups within a given $C_{60}X_{2m}$ family. Each subgroup includes isomers containing the same number of adjacent addends (NAX). As can be seen, for a given value of the X_i^j index, the smaller NAX the more stable the corresponding isomer, which is the consequence of the smaller steric hindrance. It can also be seen that the energy penalty per adjacent addend is roughly independent of NAX. However, it depends significantly on the nature of the X addend: in general, the smaller the addend the smaller the penalty, which is again the consequence of the smaller steric hindrance. Figure 1 indicates with full symbols the structures that have been experimentally synthesized.[48,57,62,92] As can be seen, they generally correspond to the lowest-energy isomers, irrespective of NAX. Within each NAX subgroup, in most cases the observed structure corresponds to the lowest value of X_i^j, thus suggesting that this index catches the essential features that determine the relative stability of the different isomers.

To generalize this idea to all possible isomers, that is, irrespective of NAX, one has thus to account for steric hindrance. The above results suggest that one could in principle use a universal steric hindrance factor that is directly proportional to NAX and does not depend on any other factor. With this idea in mind, we define the *exohedral fullerene stabilization index* for isomer $[i, j]$, XSI_i^j, as follows

$$XSI_i^j \equiv X_i^j + 0.2NAPP_i^j + \gamma_X NAX^j \quad (3)$$

where $NAPP_i^j$ is the effective number of pentagon adjacencies (or adjacent pentagon pairs, APPs) for the $[i, j]$ isomer and γ_X is a coefficient that accounts for the energy penalty associated with steric hindrance. As discussed in ref 91, the second term, $0.2NAPP_i^j$, accounts for cage strain effects, which are important when comparing cage isomers containing a different number of adjacent pentagons. The coefficient 0.2 corresponds to the energy penalty per APP (in units of -2β), which lies in the accepted range 19–24 kcal/mol found in previous work[65,93] and has been shown to work pretty well in predicting the relative stability of charged and endohedral fullerenes.[91] Taking into account that the bonding of X addends to adjacent pentagonal rings relaxes strain due to the change in carbon hybridization from sp^2 to sp^3, the value of $NAPP_i^j$ is determined as follows: pentagon adjacencies holding no X addends count as one each, those holding one addend count as half each, and those holding two addends do not count. The steric coefficient γ_X only depends on the chemical nature of the X addend. We have determined its value for X = H, F, Cl, Br, and CF_3 by fitting to the above formula to the energies of all $C_{60}X_4$ isomers lying less than 20 kcal/mol above the energy of the most stable isomer. Separate fits were performed for the different types of addends, X = H, F, Cl, Br, and CF_3 (see section 1 of the Supporting Information for details). The resulting values are γ_H = 0.22, γ_F = 0.23, γ_{Cl} = 0.28, γ_{Br} = 0.31, and γ_{CF_3} = 0.33 (in units of -2β). As expected, the larger the addend size, the larger the value of γ_X (see Figure S1 in the Supporting Information). A very important aspect of eq 3 is that XSI_i^j only depends on cage connectivity and the addends distribution, that is, on the topology of the exohedral fullerene. Therefore, there is no need for electronic structure calculations or geometry optimizations.

RESULTS AND DISCUSSION

We have used the value of γ_{Cl} to calculate XSI_i^j for a large number of chlorinated fullerenes, namely, $C_{54}Cl_8$,[68] $C_{56}Cl_{12}$,[68,101] $C_{60}Cl_{12}$,[102] $C_{66}Cl_6$,[68] $C_{66}Cl_{10}$,[68,103] $C_{70}Cl_{10}$,[104] $C_{72}Cl_4$,[105−107] $C_{78}Cl_8$,[108] and $C_{80}Cl_{12}$.[109] The specific isomers

DOI: 10.1021/jacs.6b11669
J. Am. Chem. Soc. 2017, 139, 1609−1617

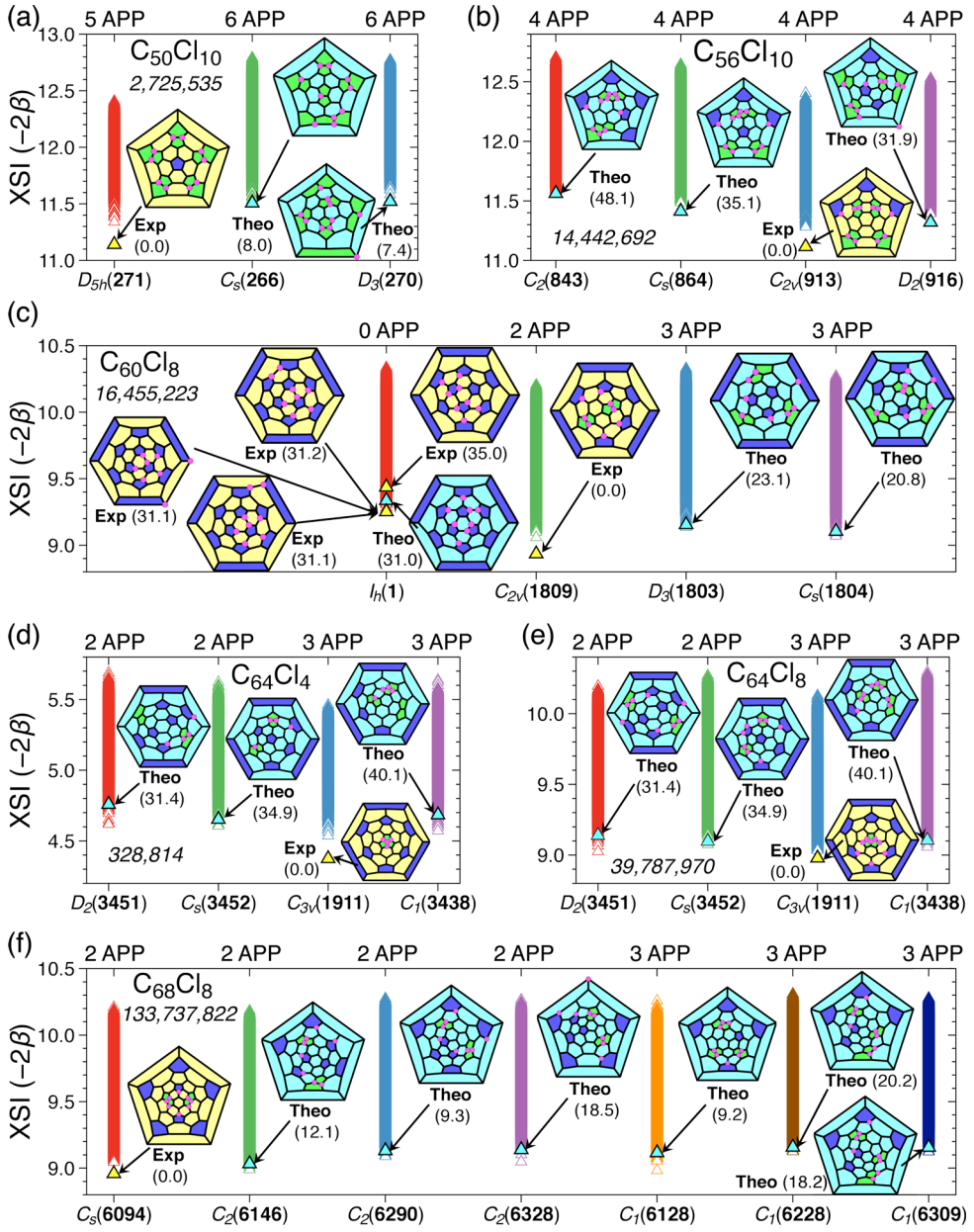

Figure 2. XSI values of chlorofullerenes with different addition patterns and different cage frameworks, $C_{2n}Cl_{2m}$ ($2n$ = 50, 56, 60, 64, 68; $2m$ = 4, 8, 10). Relative energies are given in parentheses (in kcal/mol). Exp, experimentally synthesized isomers[69,92,94−99] (full yellow triangles); Theo, lowest-energy isomers for a given fullerene cage according to DFTB calculations (full cyan triangles). The latter are not shown when they coincide with the experimentally observed ones. The structures of the most stable isomers are shown by their corresponding Schlegel diagrams in which Cl atoms are represented by magenta circles, isolated pentagons are in blue, and fused pentagons are in green. Cage isomers are labeled according to the ring spiral algorithm[100] (at the bottom of each panel). The corresponding number of APPs is given on top of each panel.

for which XSI_i^j has been evaluated have been preselected by using the stepwise addition model described in the Methods section, which is in essence similar to that proposed in ref 70 but considers a much higher energy cutoff and orders of magnitude more isomers, typically tens or hundreds of millions, since the evaluation of XSI_i^j is trivial. Figure 2 shows the calculated XSI_i^j values for isomers of $C_{50}Cl_{10}$, $C_{56}Cl_{10}$, $C_{60}Cl_8$, $C_{64}Cl_4$, $C_{64}Cl_8$, and $C_{68}Cl_8$. Results for other exohedral fullerenes, as well as a magnified version of Figure 2, can be found in the Supporting Information. The number of isomers considered in each case is indicated within each panel. For the sake of clarity, the results have been split in groups corresponding to different cage isomers (only those leading to the most stable structures are shown). Each empty triangle indicates the value of XSI_i^j for a given $[i, j]$ isomer. Due to the large number of isomers that has been considered, the empty triangles lie very close to each other, giving the impression of forming a continuous vertical line. The experimentally observed isomers[69,92,94−99] are indicated by full yellow triangles and those predicted by DFTB calculations by full cyan triangles. As can be seen, the most stable isomers[69,92,94−99] usually have the lowest XSI_i^j value. For $C_{60}Cl_8$, $C_{64}Cl_4$, and $C_{64}Cl_8$, the corresponding cage structures do not contain the minimum number of adjacent pentagons allowed by topological rules. This is because the gain in π stabilization associated with the specific cage topology and location of the chlorine atoms, and

DOI: 10.1021/jacs.6b11669
J. Am. Chem. Soc. 2017, 139, 1609−1617

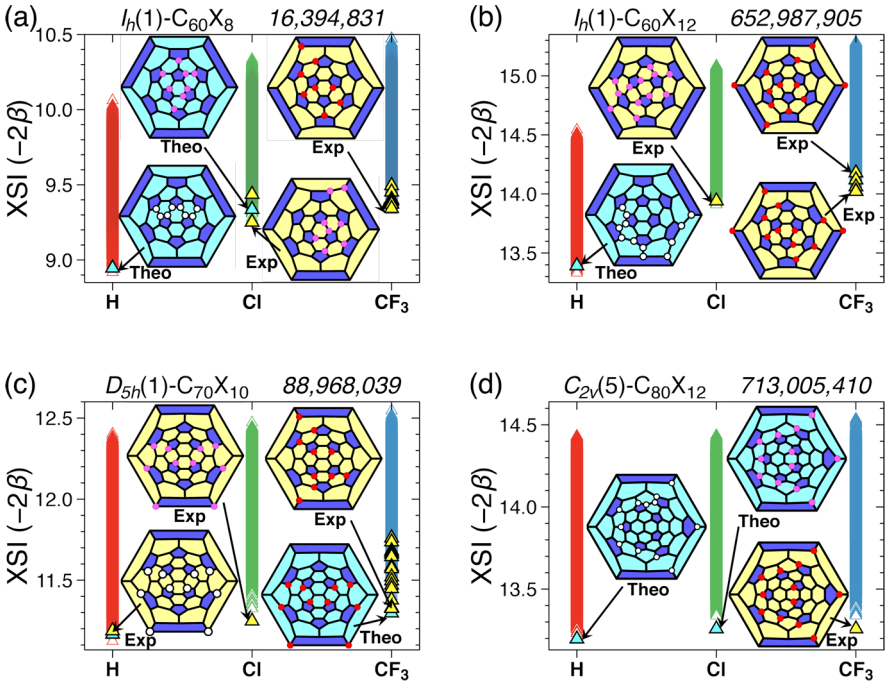

Figure 3. XSI values (open triangles) of hydrogenated, chlorinated and trifluoromethylated fullerenes with different addition patterns and different cage frameworks, $C_{2n}X_{2m}$ (X = H, Cl, CF_3; $2n$ = 60, 70, 80; $2m$ = 8, 10, 12). Exp, experimentally synthesized isomer[62,92,96,110,111] (full yellow triangle); Theo, lowest-energy isomer for a given fullerene cage from DFTB calculations (full cyan triangle). The structures of the most stable isomers are shown by their corresponding Schlegel diagrams, in which pentagonal rings are indicated in blue and hydrogen atoms as white circles, chlorine atoms as magenta circles, and CF_3 groups as red circles. The total number of isomers generated by the stepwise addition algorithm (with a cutoff energy of $0.8|\beta|$ at each step) is given at the top of each panel.

the strain relief resulting from the binding into pentagon-adjacency sites compensate steric hindrance. It is interesting to note that the delicate interplay between these effects leads to completely different cage structures depending of the number of addends. For instance, for $C_{60}Cl_8$, the most stable isomer has a cage with two APPs ($C_{2v}(1809)$), while for $C_{60}Cl_{12}$ (see Supporting Information), it has three ($C_s(1804)$), in agreement with the experimental findings.[102] Notice also that, contrary to chemical intuition, which would give preference to the formation of C−Cl bonds involving carbon atoms with a more pronounced sp^3-like character (e.g., those belonging to pentagon adjacencies),[66] the Cl atoms can bind the fullerene cage in pentagon−hexagon−hexagon junction sites while there are still pentagon−pentagon adjacencies available (e.g., see the experimentally observed structures of $C_{2v}(540)$-$C_{54}Cl_8$,[68] $C_2(843)$-$C_{56}Cl_{12}$,[68] $C_s(4169)$-$C_{66}Cl_{8/10}$,[68] and $C_{3v}(1911)$-$C_{64}Cl_8$[69] in the Supporting Information). Based on selected density functional theory (DFT) calculations, Tan et al.[68] have empirically suggested that this anomalous behavior should only be observed in fullerenes containing three pentagons consecutively fused together. From our XSI model, this can be easily understood by the fact that high steric hindrance is induced when chlorine atoms fully occupy the two pentagon-adjacency sites that are next to each other. In this case, steric repulsion prevails over strain relief, thus preventing full occupation of pentagon-adjacency sites.

By using eq 3, we have also investigated how the chemical nature of the X addends determines their geographical distribution on the fullerene cage. Figure 3 shows the calculated XSI_i^j values for isomers of $C_{60}X_8$, $C_{60}X_{12}$, $C_{70}X_{10}$, and $C_{80}X_{12}$, for X = H, Cl, and CF_3. In this example, we have only considered exohedral fullerene structures derived from the most stable pristine fullerene cages, namely, $I_h(1)$ for C_{60}, $D_{5h}(1)$ for C_{70}, and $C_{2v}(5)$ for C_{80}. Therefore, we are considering the isomers that can be formed in the low-temperature synthesis of exohedral fullerenes from pristine IPR fullerenes available in the lab. As can be seen in the figure, in most cases the lowest values of XSI_i^j correspond once again to the experimentally observed structures.[62,92,96,110,111] This is remarkable since the distribution of addends is completely different for H, Cl, and CF_3. For example, while for C_{60} and C_{70}, H atoms tend to cluster on specific regions of the fullerene cage, Cl atoms and CF_3 groups distribute more uniformly all over the cage, more in the latter case. This is logically the consequence of steric hindrance, which penalizes large addends to be close to each other. However, this is not a universal rule. Indeed, while for $C_{60}X_{2m}$ fullerenes, the distribution of H and Cl atoms follows the expected behavior, for $C_{70}X_{10}$ fullerenes the experimentally found regioisomers have the same structure for both H and Cl addends. This structure is also one of the most stable ones for CF_3 addends. For $C_{80}X_{12}$ fullerenes, the most stable structures for X = Cl and X = CF_3 are also identical. Therefore, as in the examples discussed above, it is the interplay between steric hindrance and π delocalization that dictates the addends distribution (in these cases, strain does not play any role because we are only considering IPR structures). We note that although the examples shown in Figure 3 correspond to IPR cages, the above discussion is also valid for non-IPR cages. For example, the variation of addition patterns from hydrogenation to chlorination has also been observed in experiments[102,112,113] for the non-IPR $C_{2v}(1809)$-$C_{60}X_8$ (X = H,[112] Cl[102,113]), which is correctly predicted by the XSI model (see section 3 of the Supporting Information).

DOI: 10.1021/jacs.6b11669
J. Am. Chem. Soc. 2017, 139, 1609−1617

The effect of the nature of addends on the addition patterns has been discussed in early theoretical work on $C_{60}X_2$ (X = H, F, Cl, Br, and I).[62,114] It has been shown that the *ortho* addition product (in which two addends are adjacent) is preferred for smaller addends (X = H and F) while the *para* product (in which two addends are on the *para* position of a hexagonal ring) is favored for bigger addends (X = Cl, Br, and I). For the same reason, adjacent additions are very rarely found in perfluoroalkylfullerenes ($X = C_{2x}F_{2x+1}$).[62] The combination of steric hindrance and strain relief effects, as resulting from the XSI model, allows us to understand the interesting observation that all perfluoroalkylfullerenes synthesized so far have an IPR cage:[62] non-IPR cages would favor addition on pentagon adjacency sites in order to release strain, but this is amply compensated by the high steric repulsion between the bulky perfluoroalkyl groups.

We would also like to note that the XSI model is able to predict the most stable structures generated under both thermodynamic and kinetic conditions. For instance, the reported experimental structure of $C_{2v}(1809)$-$C_{60}Cl_8$ has been obtained in high temperature experiments,[102] which allows the system to explore the whole potential energy surface and thus reach the global minimum (thermodynamic conditions). In this case, the formed isomer has the lowest value of XSI_i^j (see Figure 2c). Structures of $I_h(1)$-$C_{60}Cl_8$ lying at significantly higher energies (>30 kcal/mol) have been synthesized in solution,[92,96,115] that is, in a low temperature environment, so that the observed structures correspond to local minima of the potential energy surface (kinetic origin). These structures have the lowest XSI_i^j values within the $I_h(1)$-$C_{60}Cl_8$ family (see Figure 2c) and, therefore, restricting the application of the XSI model to a particular cage isomer also leads to the correct prediction. The model also works very well in predicting the kinetically controlled products of perfluoromethylfullerenes (see Figure 3c).

Finally, it is important to emphasize that the XSI model does a good job even for exohedral fullerenes with large cages ($2n$ = 90−108) containing a large number of addends ($2m$ = 14−24), for example, those produced in recent experiments[116] (see section 4 in the Supporting Information). In fact, the only limiting factor is the value of the m/n ratio, that is, the coverage of the fullerene cage, which cannot be very large. Indeed, a high degree of derivatization (large coverage) usually leads to a substantial deformation of the carbon cage (see Figure S18 in the Supporting Information), hence to a significant distortion of the π system, which cannot be described any more by simple Hückel approximations. Our results show that, as a rule of thumb, the XSI model works pretty well for m/n smaller than ~1/4. For larger values of this ratio, the model performs progressively worse, but it is still able to identify the experimentally observed isomers among those with the lowest XSI values.

CONCLUSION AND PERSPECTIVES

Understanding the basic rules that govern the relative stability of exohedral fullerenes $C_{2n}X_{2m}$ as a function of the number and chemical nature of the X addends and the cage characteristics is a difficult task due to the large number of possible isomeric forms associated with a given value of n and m. This is a serious limitation to understand the outcomes of experiments performed at high temperature, where in principle all topologically allowed isomeric forms are energetically accessible and standard chemical reasoning cannot be applied. For the same reasons, quantum chemistry calculations, even at the lowest possible level, are unpractical. In this work, we have proposed a simple model, exclusively based on the topology of the exohedral species, that allows one to easily predict the most stable structures, that is, the ones observed in such experiments, with a small margin of error. The model incorporates (i) the effect of π stabilization, through the diagonalization of the connectivity matrix corresponding to the derivatized fullerene cage topology, (ii) the strain associated with the presence of adjacent pentagonal rings, by the counting of these adjacencies, and (iii) the effect of steric hindrance, by the counting of X pairs bonded to adjacent sites. No iterative electronic structure calculations or geometry optimizations are needed. In spite of its simplicity, the model captures the subtleties of the interplay among these three factors and is able to explain, for example, the formation of non-IPR exohedral fullerenes while their pristine fullerene counterparts follow the usual IPR rule, the appearance of more pentagon−pentagon adjacencies than predicted by the PAPR, the changes in regioisomer stability due to the chemical nature of the X addends, and the variations in fullerene cage stability with the number of addends. In many cases, π stabilization, strain, and steric hindrance go in different directions, and it is difficult to predict which one would dominate by using standard rule-of-thumb concepts. Our model, though simple, incorporates the very minimum information that is required to perform meaningful predictions and, therefore, can be used as a reliable prescreening tool to identify the most stable isomeric forms of exohedral fullerenes.

In the future, it would be interesting to generalize the XSI model to nonclassical cage forms and more complex addends. In the case of exohedral fullerenes with cages containing heptagonal[117−119] or tetragonal[120,121] rings, additional strain terms related to pentagon−heptagon or pentagon−tetragon adjacencies should be incorporated, which requires parametrization of a sufficiently large number of DFT or semiempirical calculations but does not imply any significant reformulation. Likewise, considering more complex addends, such as CH_3, C_2F_5, phenyl, etc., requires the evaluation of their corresponding steric coefficients γ_X following a strategy similar to that described in the present work. For fullerene derivatives with more than one kind of addend,[122] additional steric coefficients should be evaluated in order to account for the interactions between different chemical groups, but again this would not introduce any unsurmountable complication. Similarly, extending the model to study the exohedral functionalization of endohedral metallofullerenes[62] should not pose any major problem. Nevertheless, the model may not work as it is and may require substantial modifications for exohedral fullerenes containing very flexible addends with complex conformations or chemical groups involving hydrogen bonding (such as OH, NH_2). Work along these lines is already in progress in our laboratory.

METHODS

XSI Evaluation and Isomer Notation. The connectivity matrix has been diagonalized by using the cyclic Jacobi method. The numbering of all fullerene isomers follows Fowler−Manolopoulos ring spiral algorithm.[100] Note that, as a convention,[123] non-IPR isomers are numbered by sorting the spiral codes among all possible isomers of a given fullerene size, while IPR isomers are numbered among all possible IPR isomers only.

Stepwise Addition Procedure for Isomer Selection. We start from the lowest-energy cage isomers of pristine fullerene whose structures are connected by Stone−Wales transformations.[124] Then,

DOI: 10.1021/jacs.6b11669
J. Am. Chem. Soc. 2017, 139, 1609−1617

for each cage isomer i, we calculate the XSI_i^j values for all regioisomers j of $C_{2n}X_{2m}$ that are generated using the following stepwise addition model:

1. We start with $C_{2n}X_2$ considering all possible regioisomers. The enumeration and identification of regioisomers are based on the minimal labeling paths[125,126] of the graph of fullerene cage. We select the isomers with the lowest XSI_i^j values within an energy range of $0.8|\beta|$ (ca. 40−50 kcal mol^{-1}).
2. We add two X addends to the lowest-XSI_i^j isomers of $C_{2n}X_2$ generated in the previous step. Among all possible addition products of $C_{2n}X_4$, we select the lowest-XSI_i^j regioisomers (with the same relative energy cutoff of $0.8|\beta|$).
3. The same procedure is repeated to obtain all regioisomers of $C_{2n}X_{2k}$ from those of $C_{2n}X_{2k-2}$ generated in the previous step until k reaches the value of m.

We have compared the results from the stepwise model and from the complete enumeration of regioisomers for $C_{64}Cl_4$ with different cage forms (see Figure 2d) and for $C_{64}Cl_8$ with cage $C_{3v}(1911)$. The comparisons validate the stepwise model, which is able to generate all the regioisomers appearing in the low-energy region (see Supporting Information).

Calculation of Relative Isomer Energies. The lowest-energy cage isomers of pristine fullerenes have been determined at the B3LYP/6-31G(d) level.[127] To identify the most stable structures not seen in experiments, we have carried out self-consistent charge density functional tight-binding (abbreviated as DFTB for convenience)[128] calculations for the 1000 regioisomers with the lowest XSI_i^j for each cage isomer. The DFTB calculations have been performed by using the DFTB+ (version 1.2) code,[129] which makes use of the second-order expansion of the Kohn−Sham energy in terms of the charge density fluctuation. The resulting energy terms are calculated by applying the tight-binding approximation and some approximate treatments similar to semiempirical quantum chemistry methods. All total energies were computed by using the equilibrium geometries, which were fully optimized without any constraint. For fullerene systems, the DFTB method has been shown to give results in good agreement with those from DFT using the B3LYP functional.[91,130]

In addition, we have confirmed the validity of the DFTB method in predicting the relative isomer energies of exohedral fullerenes, by performing higher level DFT computations for $C_{60}Cl_8$ and $C_{64}Cl_4$ systems (see Supporting Information), each with four different cage forms (see Figure 2c,d, respectively). Using the Gaussian 09 package,[131] we have calculated B3LYP/6-31G(d) energies based on fully optimized geometries for the 500 lowest energy structures predetermined at the DFTB level.

■ ASSOCIATED CONTENT

Supporting Information

The Supporting Information is available free of charge on the ACS Publications website at DOI: 10.1021/jacs.6b11669.

Determination of the steric coefficients, magnified version of Figure 2, application of the XSI model to other exohedral fullerenes, performance of the XSI model for larger systems, performance of the stepwise model for regioisomer preselection, and comparison between DFTB and DFT results (PDF)

■ AUTHOR INFORMATION

Corresponding Authors

*yang.wang@uam.es

*fernando.martin@uam.es

ORCID

Yang Wang: 0000-0003-2540-2199

Notes

The authors declare no competing financial interest.

■ ACKNOWLEDGMENTS

The authors acknowledge allocation of computer time at the Centro de Computación Científica of the Universidad Autónoma de Madrid (CCC-UAM) and the Red Española de Supercomputación. Work was supported by the MINECO projects FIS2013-42002-R and CTQ2013-43698-P, the CAM project NANOFRONTMAG-CM ref S2013/MIT-2850, and the European COST Action CM1204 XLIC. Finacial support from the Spanish Ministry of Economy and Competitiveness - MINECO - through the María de Maeztu Programme for Units of Excellence in R&D (MDM-2014-0377) is acknowledged. S.D.-T. gratefully acknowledges the "Ramón y Cajal" program of the Spanish MINECO (RYC-2010-07019).

■ REFERENCES

(1) Franco, J. U.; Ell, J. R.; Hilton, A. K.; Hammons, J. C.; Olmstead, M. M. *Fullerenes, Nanotubes, Carbon Nanostruct.* **2009**, *17*, 349−360.
(2) Babu, S. S.; Mohwald, H.; Nakanishi, T. *Chem. Soc. Rev.* **2010**, *39*, 4021−4035.
(3) Ros, T. D.; Prato, M. *Chem. Commun.* **1999**, 663−669.
(4) Bosi, S.; Da Ros, T.; Spalluto, G.; Prato, M. *Eur. J. Med. Chem.* **2003**, *38*, 913−923.
(5) Djordjević, A.; Bogdanović, G.; Dobrić, S. *J. BUON.* **2006**, *11*, 391−404.
(6) Prato, M. *J. Mater. Chem.* **1997**, *7*, 1097−1109.
(7) Wudl, F. *J. Mater. Chem.* **2002**, *12*, 1959−1963.
(8) Nierengarten, J.-F. *New J. Chem.* **2004**, *28*, 1177−1191.
(9) Yan, W.; Seifermann, S. M.; Pierrat, P.; Brase, S. *Org. Biomol. Chem.* **2015**, *13*, 25−54.
(10) Bosi, S.; Da Ros, T.; Spalluto, G.; Balzarini, J.; Prato, M. *Bioorg. Med. Chem. Lett.* **2003**, *13*, 4437−4440.
(11) Marchesan, S.; Da Ros, T.; Spalluto, G.; Balzarini, J.; Prato, M. *Bioorg. Med. Chem. Lett.* **2005**, *15*, 3615−3618.
(12) Marcorin, G. L.; Da Ros, T.; Castellano, S.; Stefancich, G.; Bonin, I.; Miertus, S.; Prato, M. *Org. Lett.* **2000**, *2*, 3955−3958.
(13) Dugan, L. L.; Turetsky, D. M.; Du, C.; Lobner, D.; Wheeler, M.; Almli, C. R.; Shen, C. K.-F.; Luh, T.-Y.; Choi, D. W.; Lin, T.-S. *Proc. Natl. Acad. Sci. U. S. A.* **1997**, *94*, 9434−9439.
(14) Lai, Y. L.; Murugan, P.; Hwang, K. C. *Life Sci.* **2003**, *72*, 1271−1278.
(15) Gonzalez, K. A.; Wilson, L. J.; Wu, W.; Nancollas, G. H. *Bioorg. Med. Chem.* **2002**, *10*, 1991−1997.
(16) Dellinger, A.; Zhou, Z.; Lenk, R.; MacFarland, D.; Kepley, C. L. *Exp. Dermatol.* **2009**, *18*, 1079−1081.
(17) Muñoz, A.; Sigwalt, D.; Illescas, B. M.; Luczkowiak, J.; Rodríguez-Pérez, L.; Nierengarten, I.; Holler, M.; Remy, J.-S.; Buffet, K.; Vincent, S. P.; Rojo, J.; Delgado, R.; Nierengarten, J.-F.; Martín, N. *Nat. Chem.* **2016**, *8*, 50−57.
(18) Wei, X.-W.; Darwish, A. D.; Boltalina, O. V.; Hitchcock, P. B.; Street, J. M.; Taylor, R. *Angew. Chem., Int. Ed.* **2001**, *40*, 2989−2992.
(19) Burley, G. A.; Avent, A. G.; Boltalina, O. V.; Gol'dt, I. V.; Guldi, D. M.; Marcaccio, M.; Paolucci, F.; Paolucci, D.; Taylor, R. *Chem. Commun.* **2003**, 148−149.
(20) Burley, G. A.; Avent, A. G.; Boltalina, O. V.; Drewello, T.; Goldt, I. V.; Marcaccio, M.; Paolucci, F.; Paolucci, D.; Street, J. M.; Taylor, R. *Org. Biomol. Chem.* **2003**, *1*, 2015−2023.
(21) Baffreau, J.; Leroy-Lhez, S.; Vân Anh, N.; Williams, R. M.; Hudhomme, P. *Chem. - Eur. J.* **2008**, *14*, 4974−4992.
(22) Roncali, J. *Chem. Soc. Rev.* **2005**, *34*, 483−495.
(23) Mi, D.; Kim, J.-H.; Kim, H. U.; Xu, F.; Hwang, D.-H. *J. Nanosci. Nanotechnol.* **2014**, *14*, 1064−1084.
(24) Nakamura, Y.; Kato, S.-I. *Chem. Rec.* **2011**, *11*, 77−94.
(25) Taylor, R. *J. Fluorine Chem.* **2004**, *125*, 359−368.
(26) Kornev, A. B.; Khakina, E. A.; Troyanov, S. I.; Kushch, A. A.; Peregudov, A.; Vasilchenko, A.; Deryabin, D. G.; Martynenko, V. M.; Troshin, P. A. *Chem. Commun.* **2012**, *48*, 5461−5463.

DOI: 10.1021/jacs.6b11669
J. Am. Chem. Soc. 2017, 139, 1609−1617

(27) Yurkova, A. A.; Khakina, E. A.; Troyanov, S. I.; Chernyak, A.; Shmygleva, L.; Peregudov, A. S.; Martynenko, V. M.; Dobrovolskiy, Y. A.; Troshin, P. A. *Chem. Commun.* **2012**, *48*, 8916−8918.
(28) Khakina, E. A.; Yurkova, A. A.; Peregudov, A. S.; Troyanov, S. I.; Trush, V. V.; Vovk, A. I.; Mumyatov, A. V.; Martynenko, V. M.; Balzarini, J.; Troshin, P. A. *Chem. Commun.* **2012**, *48*, 7158−7160.
(29) Yan, P.; Tian, C.-B.; Gao, C.-L.; Zhang, Q.; Zhan, Z.-P.; Xie, S.-Y.; Lin, M.; Huang, R.-B.; Zheng, L.-S. *Tetrahedron* **2014**, *70*, 6776−6780.
(30) Khakina, E. A.; Yurkova, A. A.; Novikov, A. V.; Piven, N. P.; Chernyak, A. V.; Peregudov, A. S.; Troshin, P. A. *Mendeleev Commun.* **2014**, *24*, 211−213.
(31) Khakina, E. A.; Peregudov, A. S.; Yurkova, A. A.; Piven, N. P.; Shestakov, A. F.; Troshin, P. A. *Tetrahedron Lett.* **2016**, *57*, 1215−1219.
(32) Xie, J. R.-H.; Zhao, J.; Sun, G.; Cioslowski, J. *J. Comput. Theor. Nanosci.* **2007**, *4*, 142−146.
(33) Burley, G. A.; Avent, A. G.; Gol'dt, I. V.; Hitchcock, P. B.; Al-Matar, H.; Paolucci, D.; Paolucci, F.; Fowler, P. W.; Soncini, A.; Street, J. M.; Taylor, R. *Org. Biomol. Chem.* **2004**, *2*, 319−329.
(34) Burley, G. A. *Angew. Chem., Int. Ed.* **2005**, *44*, 3176−3178.
(35) Strobel, P.; Riedel, M.; Ristein, J.; Ley, L.; Boltalina, O. *Diamond Relat. Mater.* **2005**, *14*, 451−458.
(36) Okino, F.; Yajima, S.; Suganuma, S.; Mitsumoto, R.; Seki, K.; Touhara, H. *Synth. Met.* **1995**, *70*, 1447−1448.
(37) Liu, N.; Touhara, H.; Okino, F.; Kawasaki, S.; Nakacho, Y. *J. Electrochem. Soc.* **1996**, *143*, 2267−2272.
(38) Iglesias-Groth, S.; Cataldo, F. Fulleranes and Carbon Nanostructures in the Interstellar Medium. *Fulleranes: The Hydrogenated Fullerenes*, 1st ed.; Springer: Dordrecht, the Netherlands, 2010; Vol. 2.
(39) Zhang, Y.; Kwok, S. *Earth, Planets Space* **2013**, *65*, 1069−1081.
(40) Becker, L.; Bada, J. L.; Winans, R. E.; Bunch, T. E. *Nature* **1994**, *372*, 507−507.
(41) Farhat, S.; Scott, C. D. *J. Nanosci. Nanotechnol.* **2006**, *6*, 1189−1210.
(42) Murayama, H.; Tomonoh, S.; Alford, J. M.; Karpuk, M. E. *Fullerenes, Nanotubes, Carbon Nanostruct.* **2005**, *12*, 1−9.
(43) Takehara, H.; Fujiwara, M.; Arikawa, M.; Diener, M. D.; Alford, J. M. *Carbon* **2005**, *43*, 311−319.
(44) Peters, G.; Jansen, M. *Angew. Chem., Int. Ed. Engl.* **1992**, *31*, 223−224.
(45) Jansen, M.; Peters, G.; Wagner, N. *Z. Anorg. Allg. Chem.* **1995**, *621*, 689−693.
(46) Darwish, A. D.; Taylor, R. Separation, characterisation and properties of highly hydrogenated [60]fullerene. *Functionalized fullerenes: proceedings of the international symposium*; Electrochemical Society: Pennington, NJ, 2000; Vol 9; pp 179−185.
(47) Wågberg, T.; Hedenström, M.; Talyzin, A. V.; Sethson, I.; Tsybin, Y. O.; Purcell, J. M.; Marshall, A. G.; Noréus, D.; Johnels, D. *Angew. Chem., Int. Ed.* **2008**, *47*, 2796−2799.
(48) Boltalina, O. V.; Darwish, A. D.; Street, J. M.; Taylor, R.; Wei, X.-W. *J. Chem. Soc., Perkin Trans Trans. 2* **2002**, 251−256.
(49) Troshin, P. A.; Kolesnikov, D.; Burtsev, A. V.; Lubovskaya, R. N.; Denisenko, N. I.; Popov, A. A.; Troyanov, S. I.; Boltalina, O. V. *Fullerenes, Nanotubes, Carbon Nanostruct.* **2003**, *11*, 47−60.
(50) Averdung, J.; Torres-Garcia, G.; Luftmann, H.; Schlachter, I.; Mattay, J. *Fullerene Sci. Technol.* **1996**, *4*, 633−654.
(51) Filippone, S.; Maroto, E. E.; Martín-Domenech, A.; Suarez, M.; Martín, N. *Nat. Chem.* **2009**, *1*, 578−582.
(52) Marco-Martínez, J.; Marcos, V.; Reboredo, S.; Filippone, S.; Martín, N. *Angew. Chem.* **2013**, *125*, 5219−5223.
(53) González, B.; Herrera, A.; Illescas, B.; Martín, N.; Martínez, R.; Moreno, F.; Sánchez, L.; Sánchez, A. *J. Org. Chem.* **1998**, *63*, 6807−6813.
(54) Wang, G.-W.; Yang, H.-T.; Wu, P.; Miao, C.-B.; Xu, Y. *J. Org. Chem.* **2006**, *71*, 4346−4348.
(55) Brough, P.; Klumpp, C.; Bianco, A.; Campidelli, S.; Prato, M. *J. Org. Chem.* **2006**, *71*, 2014−2020.
(56) Hirsch, A.; Brettreich, M. *Fullerenes: Chemistry and Reactions*; Wiley-VCH Verlag GmbH & Co. KGaA: Weinheim, Germany, 2004; pp 185−211.
(57) Cataldo, F., Iglesias-Groth, S., Eds., *Fulleranes: The Hydrogenated Fullerenes*; Springer Netherlands: Dordrecht, the Netherlands, 2010; pp 171−202.
(58) Goryunkov, A. A.; Ovchinnikova, N. S.; Trushkov, I. V.; Yurovskaya, M. A. *Russ. Chem. Rev.* **2007**, *76*, 289−312.
(59) Troyanov, S. I.; Kemnitz, E. *Curr. Org. Chem.* **2012**, *16*, 1060−1078.
(60) Boltalina, O. V. *J. Fluorine Chem.* **2000**, *101*, 273−278.
(61) Troyanov, S. I.; Kemnitz, E. *Eur. J. Org. Chem.* **2005**, *2005*, 4951−4962.
(62) Boltalina, O. V.; Popov, A. A.; Kuvychko, I. V.; Shustova, N. B.; Strauss, S. H. *Chem. Rev.* **2015**, *115*, 1051−1105.
(63) Kroto, H. W. *Nature* **1987**, *329*, 529−531.
(64) Campbell, E.; Fowler, P.; Mitchell, D.; Zerbetto, F. *Chem. Phys. Lett.* **1996**, *250*, 544−548.
(65) Albertazzi, E.; Domene, C.; Fowler, P. W.; Heine, T.; Seifert, G.; Van Alsenoy, C.; Zerbetto, F. *Phys. Chem. Chem. Phys.* **1999**, *1*, 2913−2918.
(66) Tan, Y.-Z.; Xie, S.-Y.; Huang, R.-B.; Zheng, L.-S. *Nat. Chem.* **2009**, *1*, 450−460.
(67) Martín, N. *Angew. Chem., Int. Ed.* **2011**, *50*, 5431−5433.
(68) Tan, Y.-Z.; Li, J.; Zhu, F.; Han, X.; Jiang, W.-S.; Huang, R.-B.; Zheng, Z.; Qian, Z.-Z.; Chen, R.-T.; Liao, Z.-J.; Xie, S.-Y.; Lu, X.; Zheng, L.-S. *Nat. Chem.* **2010**, *2*, 269−273.
(69) Shan, G.-J.; Tan, Y.-Z.; Zhou, T.; Zou, X.-M.; Li, B.-W.; Xue, C.; Chu, C.-X.; Xie, S.-Y.; Huang, R.-B.; Zhen, L.-S. *Chem. - Asian J.* **2012**, *7*, 2036−2039.
(70) Bihlmeier, A. *J. Chem. Phys.* **2011**, *135*, 044310.
(71) Kroto, H. W.; Walton, D. R. M. *Chem. Phys. Lett.* **1993**, *214*, 353−356.
(72) Fowler, P. W.; Heine, T.; Troisi, A. *Chem. Phys. Lett.* **1999**, *312*, 77−84.
(73) Fowler, P. W.; Rogers, K. M.; Somers, K. R.; Troisi, A. *J. Chem. Soc., Perkin Trans. 2* **1999**, 2023−2027.
(74) Birkett, P. R.; Hitchcock, P. B.; Kroto, H. W.; Taylor, R.; Walton, D. R. M. *Nature* **1992**, *357*, 479−481.
(75) Troyanov, S. I.; Troshin, P. A.; Boltalina, O. V.; Kemnitz, E. *Fullerenes, Nanotubes, Carbon Nanostruct.* **2003**, *11*, 61−77.
(76) Troshin, P. A.; Kemnitz, E.; Troyanov, S. I. *Russ. Chem. Bull.* **2004**, *53*, 2787−2792.
(77) Samokhvalova, N. A.; Khavrel', P. A.; Goryunkov, A. A.; Ioffe, I. N.; Karnatsevich, V. L.; Sidorov, L. N.; Kemnitz, E.; Troyanova, S. I. *Russ. Chem. Bull.* **2008**, *57*, 2526−2534.
(78) Troyanov, S. I.; Goryunkov, A. A.; Dorozhkin, E. I.; Ignat'eva, D. V.; Tamm, N. B.; Avdoshenko, S. M.; Ioffe, I. N.; Markov, V. Y.; Sidorov, L. N.; Scheurel, K.; Kemnitz, E. *J. Fluorine Chem.* **2007**, *128*, 545−551.
(79) Avdoshenko, S. M.; Goryunkov, A. A.; Ioffe, I. N.; Ignat'eva, D. V.; Sidorov, L. N.; Pattison, P.; Kemnitz, E.; Troyanov, S. I. *Chem. Commun.* **2006**, 2463−2465.
(80) Ignat'eva, D. V.; Goryunkov, A. A.; Tamm, N. B.; Ioffe, I. N.; Sidorov, L. N.; Troyanov, S. I. *New J. Chem.* **2013**, *37*, 299−302.
(81) Rogers, K. M.; Fowler, P. W. *Chem. Commun.* **1999**, 2357−2358.
(82) Wang, W.-W.; Dang, J.-S.; Zheng, J.-J.; Zhao, X. *J. Phys. Chem. C* **2012**, *116*, 17288−17293.
(83) Sheka, E. F. *J. Exp. Theor. Phys.* **2010**, *111*, 397−414.
(84) Cahill, P. A.; Rohlfing, C. M. *Tetrahedron* **1996**, *52*, 5247−5256.
(85) Clare, B. W.; Kepert, D. L. *J. Phys. Chem. Solids* **1997**, *58*, 1815−1821.
(86) Van Lier, G.; Cases, M.; Ewels, C. P.; Taylor, R.; Geerlings, P. *J. Org. Chem.* **2005**, *70*, 1565−1579.
(87) Ewels, C. P.; Van Lier, G.; Geerlings, P.; Charlier, J.-C. *J. Chem. Inf. Model.* **2007**, *47*, 2208−2215.
(88) Bihlmeier, A.; Tew, D. P.; Klopper, W. *J. Chem. Phys.* **2008**, *129*, 114303.

DOI: 10.1021/jacs.6b11669
J. Am. Chem. Soc. 2017, 139, 1609−1617

(89) Gao, C.-l.; Abella, L.; Tan, Y.-Z.; Wu, X.-Z.; Rodríguez-Fortea, A.; Poblet, J. M.; Xie, S.-Y.; Huang, R.-B.; Zheng, L.-S. *Inorg. Chem.* **2016**, *55*, 6861−6865.
(90) Addicoat, M. A.; Page, A. J.; Brain, Z. E.; Flack, L.; Morokuma, K.; Irle, S. *J. Chem. Theory Comput.* **2012**, *8*, 1841−1851.
(91) Wang, Y.; Díaz-Tendero, S.; Alcamí, M.; Martín, F. *Nat. Chem.* **2015**, *7*, 927−934.
(92) Kuvychko, I. V.; Streletskii, A. V.; Shustova, N. B.; Seppelt, K.; Drewello, T.; Popov, A. A.; Strauss, S. H.; Boltalina, O. V. *J. Am. Chem. Soc.* **2010**, *132*, 6443−6462.
(93) Fowler, P. W.; Manolopoulos, D. E. *Nature* **1992**, *355*, 428−430.
(94) Xie, S.-Y.; Gao, F.; Lu, X.; Huang, R.-B.; Wang, C.-R.; Zhang, X.; Liu, M.-L.; Deng, S.-L.; Zheng, L.-S. *Science* **2004**, *304*, 699−699.
(95) Tan, Y.-Z.; Han, X.; Wu, X.; Meng, Y.-Y.; Zhu, F.; Qian, Z.-Z.; Liao, Z.-J.; Chen, M.-H.; Lu, X.; Xie, S.-Y.; Huang, R.-B.; Zheng, L.-S. *J. Am. Chem. Soc.* **2008**, *130*, 15240−15241.
(96) Troshin, P. A.; Popkov, O.; Lyubovskaya, R. N. *Fullerenes, Nanotubes, Carbon Nanostruct.* **2003**, *11*, 165−185.
(97) Liang, H.; Dai, K.; Peng, R.-F.; Chu, S.-J. *Chem. - Eur. J.* **2014**, *20*, 15742−15745.
(98) Han, X.; Zhou, S.-J.; Tan, Y.-Z.; Wu, X.; Gao, F.; Liao, Z.-J.; Huang, R.-B.; Feng, Y.-Q.; Lu, X.; Xie, S.-Y.; Zheng, L.-S. *Angew. Chem., Int. Ed.* **2008**, *47*, 5340−5343.
(99) Amsharov, K. Y.; Ziegler, K.; Mueller, A.; Jansen, M. *Chem. - Eur. J.* **2012**, *18*, 9289−9293.
(100) Fowler, P.; Manolopoulos, D. E. *An Atlas of Fullerenes*; Clarendon Press: Oxford, U.K., 1995.
(101) Ziegler, K.; Mueller, A.; Amsharov, K. Y.; Jansen, M. *Chem. - Asian J.* **2011**, *6*, 2412−2418.
(102) Tan, Y.-Z.; Liao, Z.-J.; Qian, Z.-Z.; Chen, R.-T.; Wu, X.; Liang, H.; Han, X.; Zhu, F.; Zhou, S.-J.; Zheng, Z.; Lu, X.; Xie, S.-Y.; Huang, R.-B.; Zheng, L.-S. *Nat. Mater.* **2008**, *7*, 790−794.
(103) Gao, C.-L.; Li, X.; Tan, Y.-Z.; Wu, X.-Z.; Zhang, Q.; Xie, S.-Y.; Huang, R.-B. *Angew. Chem., Int. Ed.* **2014**, *53*, 7853−7855.
(104) Tan, Y.-Z.; Li, J.; Du, M.-Y.; Lin, S.-C.; Xie, S.-Y.; Lu, X.; Huang, R.-B.; Zheng, L.-S. *Chem. Sci.* **2013**, *4*, 2967−2970.
(105) Ziegler, K.; Mueller, A.; Amsharov, K. Y.; Jansen, M. *J. Am. Chem. Soc.* **2010**, *132*, 17099−17101.
(106) Tan, Y.-Z.; Zhou, T.; Bao, J.; Shan, G.-J.; Xie, S.-Y.; Huang, R.-B.; Zheng, L.-S. *J. Am. Chem. Soc.* **2010**, *132*, 17102−17104.
(107) Martín, N. *Angew. Chem., Int. Ed.* **2011**, *50*, 5431−5433.
(108) Tan, Y.-Z.; Li, J.; Zhou, T.; Feng, Y.-Q.; Lin, S.-C.; Lu, X.; Zhan, Z.-P.; Xie, S.-Y.; Huang, R.-B.; Zheng, L.-S. *J. Am. Chem. Soc.* **2010**, *132*, 12648−12652.
(109) Simeonov, K. S.; Amsharov, K. Y.; Jansen, M. *Chem. - Eur. J.* **2009**, *15*, 1812−1815.
(110) Spielmann, H. P.; Weedon, B. R.; Meier, M. S. *J. Org. Chem.* **2000**, *65*, 2755−2758.
(111) Birkett, P. R.; Avent, A. G.; Darwish, A. D.; Kroto, H. W.; Taylor, R.; Walton, D. R. M. *J. Chem. Soc., Chem. Commun.* **1995**, 683−684.
(112) Weng, Q.-H.; He, Q.; Liu, T.; Huang, H.-Y.; Chen, J.-H.; Gao, Z.-Y.; Xie, S.-Y.; Lu, X.; Huang, R.-B.; Zheng, L.-S. *J. Am. Chem. Soc.* **2010**, *132*, 15093−15095.
(113) Chen, R.-T.; Zhou, S.-J.; Liang, H.; Qian, Z.-Z.; Li, J.-M.; He, Q.; Zhang, L.; Tan, Y.-Z.; Han, X.; Liao, Z.-J.; Weng, W.-Z.; Xie, S.-Y.; Huang, R.-B.; Zheng, L.-S. *J. Phys. Chem. C* **2009**, *113*, 16901−16905.
(114) Dixon, D. A.; Matsuzawa, N.; Fukunaga, T.; Tebbe, F. N. *J. Phys. Chem.* **1992**, *96*, 6107−6110.
(115) Ziegler, K.; Amsharov, K. Y.; Jansen, M. *Z. Naturforsch., B: J. Chem. Sci.* **2012**, *67*, 1091−1097.
(116) Wang, S.; Yang, S.; Kemnitz, E.; Troyanov, S. I. *Inorg. Chem.* **2016**, *55*, 5741−5743.
(117) Tan, Y.-Z.; Chen, R.-T.; Liao, Z.-J.; Li, J.; Zhu, F.; Lu, X.; Xie, S.-Y.; Li, J.; Huang, R.-B.; Zheng, L.-S. *Nat. Commun.* **2011**, *2*, 420.
(118) Yang, S.; Wang, S.; Kemnitz, E.; Troyanov, S. I. *Angew. Chem., Int. Ed.* **2014**, *53*, 2460−2463.
(119) Ioffe, I. N.; Yang, S.; Wang, S.; Kemnitz, E.; Sidorov, L. N.; Troyanov, S. I. *Chem. - Eur. J.* **2015**, *21*, 4904−4907.
(120) Qian, W.; Bartberger, M. D.; Pastor, S. J.; Houk, K. N.; Wilkins, C. L.; Rubin, Y. *J. Am. Chem. Soc.* **2000**, *122*, 8333−8334.
(121) Qian, W.; Chuang, S.-C.; Amador, R. B.; Jarrosson, T.; Sander, M.; Pieniazek, S.; Khan, S. I.; Rubin, Y. *J. Am. Chem. Soc.* **2003**, *125*, 2066−2067.
(122) Matsuo, Y.; Nakamura, E. *Chem. Rev.* **2008**, *108*, 3016−3028.
(123) Popov, A. A.; Yang, S.; Dunsch, L. *Chem. Rev.* **2013**, *113*, 5989−6113.
(124) Stone, A. J.; Wales, D. J. *Chem. Phys. Lett.* **1986**, *128*, 501−503.
(125) Shao, Y.; Jiang, Y. *Chem. Phys. Lett.* **1995**, *242*, 191−195.
(126) Fowler, P. W.; Horspool, D.; Myrvold, W. *Chem. - Eur. J.* **2007**, *13*, 2208−2217.
(127) Wang, Y.; Alcamí, M.; Martín, F. Clusters and Fullerenes. In *Handbook of Nanophysics*; Sattler, K. D., Ed.; Taylor & Francis Publisher (CRC Press): London, 2010; Vol. *2*, Chapter 25, pp 1−23.
(128) Elstner, M.; Porezag, D.; Jungnickel, G.; Elsner, J.; Haugk, M.; Frauenheim, T.; Suhai, S.; Seifert, G. *Phys. Rev. B: Condens. Matter Mater. Phys.* **1998**, *58*, 7260−7268.
(129) Aradi, B.; Hourahine, B.; Frauenheim, T. *J. Phys. Chem. A* **2007**, *111*, 5678−5684.
(130) Wang, Y.; Díaz-Tendero, S.; Martín, F.; Alcamí, M. *J. Am. Chem. Soc.* **2016**, *138*, 1551−1560.
(131) Frisch, M. J.; Trucks, G. W.; Schlegel, H. B.; Scuseria, G. E.; Robb, M. A.; Cheeseman, J. R.; Scalmani, G.; Barone, V.; Mennucci, B.; Petersson, G. A.; Nakatsuji, H.; Caricato, M.; Li, X.; Hratchian, H. P.; Izmaylov, A. F.; Bloino, J.; Zheng, G.; Sonnenberg, J. L.; Hada, M.; Ehara, M.; Toyota, K.; Fukuda, R.; Hasegawa, J.; Ishida, M.; Nakajima, T.; Honda, Y.; Kitao, O.; Nakai, H.; Vreven, T.; Montgomery, J. A., Jr.; Peralta, J. E.; Ogliaro, F.; Bearpark, M.; Heyd, J. J.; Brothers, E.; Kudin, K. N.; Staroverov, V. N.; Kobayashi, R.; Normand, J.; Raghavachari, K.; Rendell, A.; Burant, J. C.; Iyengar, S. S.; Tomasi, J.; Cossi, M.; Rega, N.; Millam, J. M.; Klene, M.; Knox, J. E.; Cross, J. B.; Bakken, V.; Adamo, C.; Jaramillo, J.; Gomperts, R.; Stratmann, R. E.; Yazyev, O.; Austin, A. J.; Cammi, R.; Pomelli, C.; Ochterski, J. W.; Martin, R. L.; Morokuma, K.; Zakrzewski, V. G.; Voth, G. A.; Salvador, P.; Dannenberg, J. J.; Dapprich, S.; Daniels, A. D.; Farkas, O.; Foresman, J. B.; Ortiz, J. V.; Cioslowski, J.; Fox, D. J. *Gaussian 09*, revision C.01; Gaussian, Inc.: Wallingford, CT, 2009.

DOI: 10.1021/jacs.6b11669
J. Am. Chem. Soc. 2017, 139, 1609−1617